Electronic Supplementary Information

One Spiro to Shift Them All: Tuning Fluorescent Organic Nanoparticles Emission via Steric Design

Eleonore Kurek[‡,†] Ophélie Dal Pra[‡,†] Aliocha Skrzypczak,[†] Stéphane Massip,[‡] Jonathan Daniel,[†] Mireille Blanchard-Desce,[*,†] and Chloé Grazon[*,†]

†*Univ. Bordeaux, CNRS, Bordeaux INP, ISM, UMR 5255, F-33400 Talence, France*

‡ *these authors contributed equally*

‡*Univ. Bordeaux, CNRS, INSERM, IECB, UAR 3033, F-33600 Pessac, France*

E-mail: mireille.blanchard-desce@u-bordeaux.fr; chloe.grazon@u-bordeaux.fr

Contents

1 Materials

1.1 Chemical characterizations

^{1}H and ^{13}C NMR spectra were recorded on a Bruker Avance I 300 spectrometer at 300 MHz and 75 MHz respectively or on a Bruker Avance III 600 spectrometer at 600 MHz and 150 MHz respectively. Chemical shifts (δ) are reported in ppm and residual non-deuterated solvent were used as an internal reference. Coupling constants (J) are given in Hertz. The deuterated solvents are supplied by Eurisotop (DMSO) or Sigma-Aldrich ($CDCl_3$). High-resolution mass spectra were carried out at the Centre Régional de Mesures Physiques de l'Ouest (CRMPO) in Rennes. MALDI-MS spectra were performed by the CESAMO (Bordeaux, France) on an Autoflex maX TOF mass spectrometer (Bruker Daltonics, Bremen, Germany) equipped with a frequency tripled Nd:YAG laser emitting at 355 nm. Spectra were recorded in the positive-ion mode using the reflectron and with an accelerating voltage of 19 kV. Samples were dissolved in DMSO at 1 mg/mL and 2 µL of this solution was deposited onto the sample target and vacuum-dried. The DMEM culture medium was freeze-dried and then reconstituted in pure FBS to obtain a home-made solution of DMEM+ 10% FBS 10x.

1.2 Transmission Electron Microscopy

Dry diameters of *d*FONs were determined by TEM. In short, undiluted samples were deposited on positively charged carbon-membrane coated copper grids. After removal of the sample drop and air drying of the grid, uranyl acetate (3wt%) was deposited onto the grids to contrast the objects. After removal of the contrasting agent drop and air drying of the grid, the *d*FONs were imaged on a Hitachi H7650 electron microscope (80 kV).

The images were analyzed using a Python segmentation analysis program (code available upon request and deposited on an online open access folder) to extract the mean nanoparticle diameters. The average number of dye molecules per *d*FON, denoted N, was determined from the mean nanoparticle diameter (D_{TEM}) using the equation:

$$N = \frac{4}{3} \cdot \pi \cdot (\frac{D_{TEM}}{2}) \cdot \frac{\rho}{M} \cdot N_A \quad (1)$$

where the density of the *d*FON (ρ) is assumed to be equal to 1 g cm^{-3}, M is the molecular weight of the dye and N_A the Avogadro constant.

1.3 Photophysical characterizations

The absorption and fluorescence emission spectra were respectively recorded on a Jasco V670 or on a UV5 Nano Mettler Toledo and an Edinburgh instruments FLS 1000 spectrometers. Emission of crystals made of dyes were measured on a Horiba FluoroLog 3 spectrophotometer at the magic angle (front face collection). All photophysical studies were performed at room temperature, on dye solutions prepared in spectroscopic grade solvents or on freshly prepared and air-equilibrated nanoparticle suspensions in distilled water. The solutions were placed in quartz cuvettes with an optical path length of 1 cm. All fluorescence emission spectra were corrected for a device function and recorded at 90° on samples with an absorbance of less than 0.1 at the excitation wavelength. The fluorescence quantum yield (Φ_F) was calculated relative to a reference (quinine bisulfate $\Phi_F = 0.546$ in 0.5 M H_2SO_4[1] or 4-(dicyanomethylene)-2-methyl-6-[p-(dimethyl-amino) styryl]-4H-pyran $\Phi_F = 0.437$ in EtOH[2]), using the equation:

$$\Phi_F = \Phi_{F,\text{ref}} \times \frac{\text{Grad}}{\text{Grad}_{\text{ref}}} \times \frac{n^2}{n_{\text{ref}}^2} \quad (2)$$

where $\Phi_{F,\text{ref}}$ is the fluorescence quantum yield of the reference, Grad and Grad_{ref} are the slopes of the integrated fluorescence intensity vs absorbance at the excitation wavelength for the sample and reference, respectively and n and n_{ref} are the refractive indices of the sample and reference solutions, respectively.

The molar extinction coefficients (ε_{dye}) of the dyes were determined from three inde-

pendent weighings of dye, followed by the preparation of three concentrated stock solutions in dimethyl sulfoxide (DMSO - a good solvent for all dyes), and several rounds of dilution in tetrahydrofuran (THF), resulting in at least six absorbance measurements at six different concentrations (<8% DMSO). Each molar extinction coefficient was determined by linear regression of the data, and the standard deviation from all points was calculated to estimate the measurement error.

The molar extinction coefficient of the dyes within the *d*FONs (ε_{dFONs}) was determined by freeze-drying 2mL of *d*FONs suspensions of known absorbance (A_{dFONs}), and subsequently dissolving the remaining solid in the smallest possible volume of DMSO, followed by dilution in THF, resulting in a final volume of 2mL (<8% DMSO). Using the known molar extinction coefficient of the dye in THF (ε_{dye}), the absorbance (A_{dye}) of this molecular solution was then used to determine the initial dye concentration in the *d*FONs suspension and thus the associated solid state molar extinction coefficient:

$$\varepsilon_{dFONs} = \varepsilon_{dye} \times \frac{A_{dFONs}}{A_{dye}} \tag{3}$$

The brightness of the *d*FONs is calculated using the equation:

$$B = N \times \varepsilon_{dFON} \times \Phi_F \tag{4}$$

where N is the number of dyes per *d*FONs, calculated using eq. 1, ε_{dFON} is the molar coefficient absorption of a dye in the dFONs, calculated using eq. 3 and Φ_F is the *d*FONs quantum yield (eq. 2).

The brightness per volume, B_v is simply the *d*FONs brightness divided by the volume of the nanoparticle, but can also be directly calculated using the equation:

$$B_V = \frac{\rho \times N_A}{M} \times \varepsilon \times \Phi_F \tag{5}$$

Fluorescence lifetime measurements were performed on an Edinburgh Instruments FLS1000 using a NanoLed-370 with Controler NL-C2 (both Horiba) for excitation at 370 nm. Aqueous dispersion of Ludox (30% in water, Sigma–Aldrich) was used to record the instrument response. Fluorescence decays ($I(t)$) are adjusted using the reconvolution method of the Fluoracle software. The fluorescence decays of the molecular dyes in THF were fitted with a single exponential function. The dFONs fluorescence decays in water were fitted with a sum of two exponentials:

$$I(t) = \sum_i a_i e^{-\frac{t}{\tau_i}} \tag{6}$$

Where I is the normalized fluorescence intensity, t is the delay time and a_i are the normalized pre-exponential coefficients and τ_i the individual fluorescence lifetimes.

The amplitude average fluorescence lifetime (τ_{amp}) is calculated using:

$$\tau_{\text{amp}} = \frac{\sum_i a_i \tau_i}{\sum_i a_i} \tag{7}$$

Where a_i are the normalized pre-exponential coefficients and τ_i are the individual fluorescence lifetimes.

Finally, the radiative rate (k_r) and non-radiative rate (k_{nr}) are calculated as:

$$k_r = \frac{\Phi_F}{\tau_{\text{amp}}} \tag{8}$$

$$k_{nr} = \frac{1 - \Phi_F}{\tau_{\text{amp}}} \tag{9}$$

1.4 X-ray analyses

X-ray analyses of compounds were carried out on a FR-X Rigaku diffractometer with rotating anode at monochromatic Cu-Ka radiation ($l = 1.54184$ Å) and a Pixel Hybrid detector HyPix

6000. Data collection and reduction was performed with CrysAlisPro.[3] The structure was solved by direct methods and refined using Shelx 2014 suite of programs[4] in the integrated WinGX system.[5] The positions of the H atoms were deduced from coordinates of the non-H atoms and confirmed by Fourier synthesis. The non-H atoms were refined with anisotropic temperature parameters. H atoms were included for structure factor calculations but not refined. The program Mercury[6] was used for analysis and drawing figures.

1.5 Bioimaging

COS-7 cells cells were provided by the IINS Cell Biology Facility of the University of Bordeaux and supported by the GPR BRAIN_2030. HEK-293T Human Embryonic Kidney cells were provided by the BiOf Lab (LP2N, UMR5298) of the University of Bordeaux. The cells were grown in standard conditions (DMEM Glutamax medium + 10% Fetal Bovine Serum + 1% Penicillin and Streptomycin).

Confocal microscopy was performed on the Bordeaux Imaging Center, a service unit of the CNRS-INSERM and Bordeaux University, member of the national infrastructure France BioImaging supported by the French National Research Agency (ANR-10-INBS-04). We imaged the samples with a Leica TCS SP5 upright confocal microscope (stand DM6000).

In order to limit the dilution of the nanoparticles in the cell medium upon incubation, we prepared a concentrated solution of cell nutrients to add to the *d*FONs suspension. This solution was prepared from freeze-dried Dulbecco's Modified Eagle Medium (DMEM) (initially 10mL), which was resuspended in 1mL of Fetal Bovine Serum (FBS). Then 200μL of this 10X DMEM + 100% FBS solution were added to 1.8mL of pristine *d*FON($dye{\cdot}spiC_4$), resulting in a final incubation mixture containing 9:10 diluted *d*FON($dye{\cdot}spiC_4$) (5nM), 1X DMEM, and 10% FBS. Fluorescence microscopy images were acquired on COS-7 cells after 2h of incubation with this mixture at 37°C, and 3 rinses using PBS. For HEK-293T cells, the images were acquired under wash-free conditions with different incubation times. For accumulation experiments, the cells were kept on the microscope for the entire duration of

the experiment. *d*FONs were excited with a 405 nm diode through a 60X water immersion objective (HC PL APO 63x/1,20 W CORR CS2), and their reflected fluorescence was collected with hybrid detectors. Excitation and emission wavelengths are stated in the text or figure captions for more clarity, and we made sure all acquisition parameters are kept constant in between each comparable sample.

2 Methods

2.1 Chemical synthesis

Commercially available reagents (purchased form Aldrich, Alfa, TCI or Fluorochem) were used as received. Spectroscopic grade solvents were used for photophysical characterizations: THF (Alfa Aesar, 99.7+%, unstab.), DMSO (Sigma-Aldrich, $\geq$ 99.7%), ethanol (Alfa Aesar, 90%, 5% methanol, 5% isopropanol). Reactions were monitored by thin-layer chromatography carried out on silica gel precoated aluminum sheets (60F-254). Column chromatography was performed using silica gel Si 60 (40-63 µm). For the reaction carried out under inert atmosphere, chloroform was dried on $CaCl_2$ and distilled prior to use and acetonitrile was dried on a solvent purification system.

2,7-Diiodo[alkyl-9,9-fluorene]

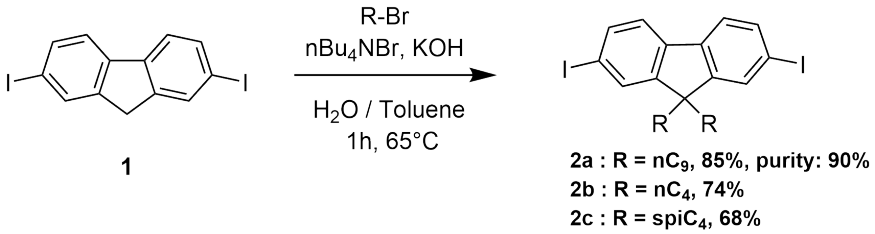

Scheme S1: Synthesis of the three 2,7-Diiodo[alkyl-9,9-fluorene]

2,7-diiodo-9,9-dinonylfluorene (**2a**) and 2,7-diiodo-9,9-dibutylfluorene (**2b**) were synthesized by adapting the procedure previously used for 2,7-diiodospiro[cyclopentane-9,9-fluorene]

(**2c**), which was obtained in a 68% yield.[7] Briefly, KOH (2.7 g, 47.8 mmol, 10 eq.) was dissolved in water (2 ml) in a 25 ml round-bottom flask. To this solution, nBu_4NBr (308 mg, 0.96 mmol, 0.2 eq.) and 1-bromononane (3.1 g, 14.8 mmol, 3.1 eq.) or 1-bromobutane (1.6 mL, 14.8 mmol, 3.1 eq.) were added and the mixture was stirred at 75°C for 30 min. A solution of 1 (2.0 g, 4.78 mmol, 1 eq.) in toluene (10 mL) was added and the mixture was further stirred at 75°C for 2h. The biphasic emulsion was cooled down to R.T, then 30 mL of water was added and the crude was extracted with dichloromethane (3 times). The organic phase was washed with water (3 times), dried over anhydrous $MgSO_4$, filtered and concentrated to dryness. The product **2a** was obtained with a purity of 90% (traces of 1-bromononane) as a partially crystallized yellow liquid without recrystallization (3.1 g, molar yield = 85%). The crude of **2b** was then recrystallized in hexane to obtain the pure product **2b** as a yellowish powder (1.86 g, molar yield 74%).

2a: ^{1}H NMR (300 MHz, $CDCl_3$) δ (ppm): 7.67-7.61 (m, 4H), 7.43 – 7.38 (dd, J = 7.7 Hz, J = 2.9 Hz, 2H), 1.88 (m, 4H), 1.47-0.96 (m, 20H), 0.85 (m, 10H), 0.57 (m, 4H).

2b: ^{1}H NMR (300 MHz, $CDCl_3$) δ (ppm): 7.67 – 7.62 (m, 4H), 7.42 – 7.38 (dd, J = 7.67 Hz, J = 2.9 Hz, 2H), 1.90 (m, 4H), 1.09 (h, J = 7.4 Hz, 4H), 0.69 (t, J = 7.3 Hz, 6H), 0.62 – 0.48 (m, 4H).

2c: ^{1}H NMR (300 MHz, $CDCl_3$) δ (ppm): 7.75 (d, J = 1.6 Hz, 2H), 7.67 (dd, J = 8.0, 1.6 Hz, 2H), 7.43 (d, J = 8.0 Hz, 2H), 2.24 – 1.95 (m, 8H).

2,7-bis(5-acid-thiophen-2-yl)-9,9-alkylfluorene carboxylic

2,7-bis(5-acid-thiophen-2-yl)-9,9-dinonylfluorene carboxylic (**3a**) or 2,7-bis(5-acidethiophen-2-yl)-9,9-dibutylfluorene carboxylic (**3b**) were synthesized following the same protocol. Compound 2a (610 mg, 90% pure, 0.81 mmol, 1 eq.), 5-carboxythiophene-2-boronic acid pinacol ester (550 mg, 2.16 mmol, 2.7 eq.), K_2CO_3 (1.3 g, 9.79 mmol, 12 eq.) and [1, 1'-bis(diphenylphosphino) ferrocene] dichloropalladium(II) ($PdCl_2$(dppf)) (15.3 mg, 0.02 mmol,

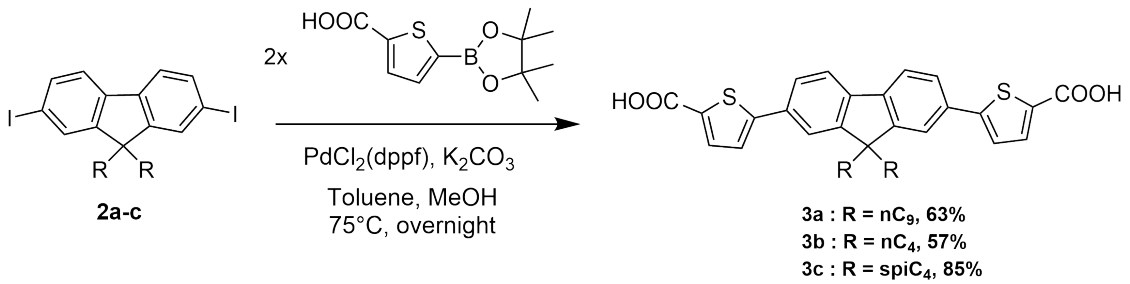

Scheme S2: Synthesis of the three 2,7-bis(5-acid-thiophen-2-yl)-9,9-alkylfluorene carboxylic

0.02 eq.) or compound 2b (500 mg, 0.94 mmol, 1 eq.), 5-carboxythiophene-2-boronic acid pinacol ester (552 mg, 2.17 mmol, 2.3 eq.), K_2CO_3 (1.3 g, 9.42 mmol, 10 eq.) and [1, 1'-bis(diphenylphosphino) ferrocene]dichloropalladium(II) ($PdCl_2$(dppf)) (15.6 mg, 0.02 mmol, 0.02 eq.) were mixed in a two-neck round-bottom flask. In a separate flask, 30 mL of distilled toluene and 20 mL of distilled methanol were combined and degassed with argon for 30 minutes. The contents of the second flask were then transferred to the first flask via a cannula under an argon atmosphere. The mixture was stirred overnight under reflux. A pale-yellow precipitate appears. The medium was cooled down to room temperature and the precipitated product was filtered and washed with toluene, HCl (1 M), water and ethanol. The products were dried to yield the pure compounds: **3a** as a pale-yellow powder (316 mg, 63%) and **3b** as a pale-yellow powder (287 mg, 57%). **3c** was synthesized previsouly with a yield of 85%.[7]

3a: ^{1}H NMR (300 MHz, DMSO-*d*6) δ (ppm): 7.90 (d, J = 8.0 Hz, 2H), 7.85 (d, J = 1.7 Hz, 2H), 7.75-7.70 (m, 4H), 7.67 (d, J = 3.9 Hz, 2H), 2.08 (m, 4H), 1.20 – 0.90 (m, 20H), 0.74 (m, 10H), 0.53 (m, 4H).

3b: ^{1}H NMR (300 MHz, DMSO-*d*6) δ (ppm): 7.91 (d, J = 8.0 Hz, 2H), 7.87 (d, J = 1.7 Hz, 2H), 7.78 – 7.65 (m, 6H), 2.12 (m, 4H), 1.04 (h, J = 7.6 Hz, 4H), 0.62 (t, J = 7.3 Hz, 6H), 0.56 – 0.43 (m, 4H).

3c: ^{1}H NMR (300 MHz, DMSO-*d*6) δ (ppm): 7.91 (d, J = 8.0 Hz, 2H), 7.83 (d, J = 1.6 Hz, 2H), 7.72 (dd, J = 7.9, 1.6 Hz, 2H), 7.65 (m, 4H), 2.31 – 2.01 (m, 8H).

2,7-bis(5-N(hydroxysuccinimide-ester-thiophen-2-yl)-9,9-dialkylfluorene

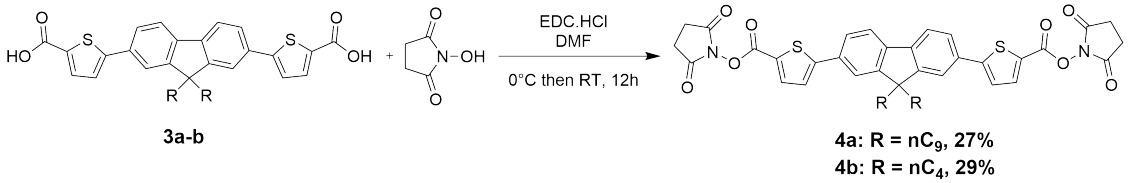

Scheme S3: Synthesis of the two 2,7-bis(5-N(hydroxysuccinimide-ester-thiophen-2-yl)-9,9-dialkylfluorene

Compounds **3a** (100 mg, 0.15 mmol, 1 eq.) or **3b** (100 mg, 0.19 mmol, 1 eq.) were weighted in a round-bottom flask and solubilized in DMF (2 mL). In another flask, EDC-HCl (144.5 mg, 0.76 mmol, 4 eq) or (114.3 mg, 0.60 mmol, 4e q) and NHS (46.4 mg, 0.40 mmol, 2,1 eq) or (36.7 mg, 0.32 mmol, 2.1 eq) were weighted, dried under vacuum, solubilized in dry DMF (4 mL) and stirred 15 min at RT. All reagents were combined and stirred at 4°C for 1 hour, followed by stirring overnight at room temperature. Then, DMF was evaporated without heating (NHS is sensitive to heat). The solution was extracted with dichloromethane and washed once with water. After drying and evaporating the organic phase, the crude was purified on silica-gel column chromatography using DCM/MeCN: 98/2 as an eluent. Product **4a** was obtained as a yellow viscous liquid (34.8 mg, 27%) and product **4b** as a pale-yellow powder (39 mg, 29%).

4a: ^{1}H NMR (300 MHz, $CDCl_3$) δ (ppm): 8.02 (d, J = 4.0 Hz, 2H), 7.77 (d, J = 7.9 Hz, 2H), 7.68 (dd, J = 8.1 Hz, 2H), 7.61(d, J = 1.6 Hz, 2H),), 7.45 (d, J = 4.0 Hz, 2H), 2.92 (s, 8H), 2.03 (m, 4H), 1.36 – 0.94 (m, 24H), 0.81 (m, 6H), 0.67 (m, 4H).

4b: ^{1}H NMR (300 MHz, $CDCl_3$) δ (ppm): : 8.02 (d, J = 4.1 Hz, 2H), 7.80 - 7,65 (m, 4H), 7.62 (d, J = 0.9 Hz, 2H), 7.45 (d, J = 4.0 Hz, 2H), 2.92 (s, 8H), 2.05 (m, 4H) 1.12 (h, J = 7.3 Hz, 4H), 0.73 – 0.58 (m, 10H).

2,7-bis(5-benzylamine thiophen-2-yl)-9,9-dinonylfluorene *dye.n*C_9 (5a) / 2,7-bis(5-benzylamine-thiophen-2-yl)-9,9-dibutylfluorene: *dye.n*C_4 (5b)

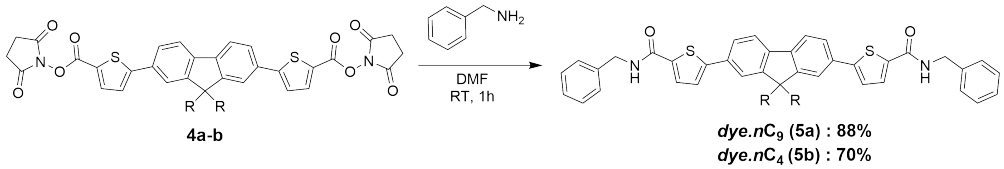

Scheme S4: Synthesis of 2,7-bis(5-benzylamine thiophen-2-yl)-9,9-dinonylfluorene *dye.n*C_9 (5a) / 2,7-bis(5-benzylamine-thiophen-2-yl)-9,9-dibutylfluorene *dye.n*C_4 (5b)

The reaction was performed in a glove box. Compound **4a** (20 mg, 0.023, 1 eq.) / compound **4b** (30 mg, 0.041 mmol, 1 eq.) was mixed with benzylamine (7.6 µL, 0.069 mmol, 3 eq) / (13.6 µL, 0.12 mmol, 3 eq) and distilled DMF (0.5 ml). The reaction was stirred for 1h at RT. DMF was evaporated and the crude was extracted with ethyl acetate and washed with water, saturated citric acid, water again, $NaHCO_3$ and water. After drying with $MgSO_4$, the product is concentrated to dryness to afford ***dye.n*$\mathbf{C_9}$ (5a)** (17.4 mg, 88%) and ***dye.n*$\mathbf{C_4}$ (5b)** (21 mg, 70%) as a pale-yellow solid. Crystals of *dye.n*C_4 were grown from a solution of dye in chloroform and ethanol, in saturated pentane atmosphere, while crystals of *dye.n*C_9 were grown from a solution in dicholoromethane slowly evaporated. **5a:** ^{1}**H NMR** (600 MHz, $CDCl_3$) δ (ppm): 7.70 (d, J = 7.9 Hz, 2H), 7.62 (dd, J = 7.9, 1.7 Hz, 2H), 7.57 (d, J = 1.7 Hz, 2H), 7.51 (d, J = 3.9 Hz, 2H), 7.41 – 7.35 (m, 8H), 7.33 - 7.29 (m, 4H), 6.25 (t, J = 5.7 Hz, 2H), 4.66 (d, J = 5.7 Hz, 4H), 2.05 – 1.95 (m, 4H), 1.18 (m, 4H), 1.12 (m, 8H), 1.05 (m, 12H), 0.80 (t, J = 7.2 Hz, 6H), 0.66 (m, 4H).

5a: ^{13}**C NMR** (150 MHz, $CDCl_3$) δ (ppm): 161.82, 152.16, 149.74, 141.10, 138.18, 136.97, 132.73, 129.34, 128.99, 128.15, 127.89, 125.36, 123.45, 120.61, 120.51, 55.56, 44.25, 40.42, 31.94, 30.05, 29.60, 29.32, 23.90, 22.75, 14.21.

5a: HRMS (ESI): *m/z* m/z $[M+H]^+$ calcd for$C_{55}H_{65}N_2O_2S_2$, z = 1, 849.4482 ; found: 849.4512.

5b: ^{1}**H NMR** (600 MHz, DMSO-*d*6) δ (ppm): 9.08 (t, J = 6.0 Hz, 2H), 7.89 (d, J = 8.0 Hz, 2H), 7.84 (d, J = 3.9 Hz, 2H), 7.82 (m, 2H), 7.71 (dd, J = 7.8, 1.7 Hz, 2H), 7.65 (d, J = 3.9 Hz, 2H), 7.39 – 7.30 (m, 8H), 7.26 (m, 2H), 4.48 (d, J = 5.9 Hz, 4H), 2.10 (m, 4H),

1.05 (q, J = 7.4 Hz, 4H), 0.63 (t, J = 7.3 Hz, 6H), 0.54 (m, 4H).

5b: ^{13}**C NMR** (150 MHz, DMSO-*d*6) δ (ppm): 160.99, 151.58, 148.00, 140.32, 139.45, 138.43, 132.34, 129.30, 128.34, 127.29, 126.86, 124.88, 124.41, 120.84, 119.96, 54.99, 42.52, 38.93, 25.79, 22.36, 13.70.

5b: HRMS (ESI): m/z $[M]^+$ calcd for $C_{45}H_{44}N_2O_2S_2$, z = 1, 708.28442; found: 708.2822.

2,7-bis(5-benzylamine-thiophen-2-yl)spiro[cyclopentane-9,9-fluorene]: *dye.spi*C_4 (5c)

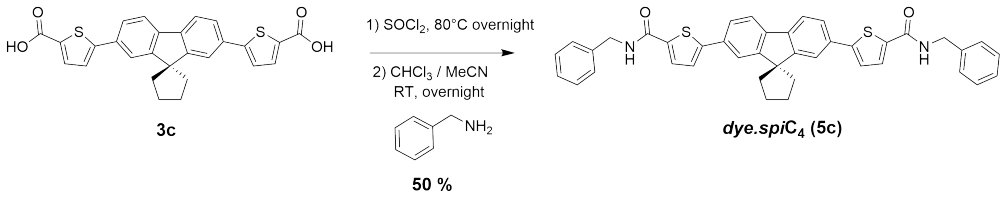

Scheme S5: Synthesis of 2,7-bis(5-benzylamine-thiophen-2-yl)spiro[cyclopentane-9,9-fluorene] : *dye.spi*C_4 (5c)

Diacid **3c** (200 mg, 0.42 mmol, 1 eq.) was dissolved into dry $SOCl_2$(16 mL) and heated to reflux overnight. The next day, $SOCl_2$ was evaporated under vacuum with two liquid nitrogen traps. The flask 1 containing the acyl chloride was entered in an argon glove box and anhydrous chloroform (20 mL) was added in the flask. In a separated flask 2, benzylamine (925 µL, 8.346 mmol, 20 eq.) was mixed with anhydrous acetonitrile (5 mL). Mixture of flask 1 was added to flask 2 and stirred overnight at RT. The light brown precipitate formed, floating on the surface of the reaction medium, was filtered and then washed with acidified water (HCl 0.1 N) three times, ethanol three times and pentane once. After being dried under reduced pressure, the product ***dye.spi*C_4 (5c)** was afforded as a pure pale-yellow solid (139 mg, 50%).

5c: ^{1}H NMR (300MHz, DMSO-*d*6) δ (ppm): 9.08 (t, J = 6.0 Hz, 2H), 7.91 (d, J = 8.0 Hz, 2H), 7.87 – 7.78 (m, 4H), 7.71 (dd, J = 7.9, 1.7 Hz, 2H), 7.65 (d, J = 3.9 Hz, 2H), 7.40

– 7.22 (m, 10H), 4.48 (d, J = 5.9 Hz, 4H), 2.27 – 2.01 (m, 8H).

5c: ^{13}C NMR (150 MHz, DMSO-*d*6) δ (ppm): 161.0, 155.0, 147.9, 139.5, 138.6, 138.5, 132.8, 129.3, 128.4, 127.3, 126.9, 124.9, 124.5, 120.8, 120.1, 57.4, 42.5, 26.4.

5c: HRMS (MALDI-TOF): m/z $[M]^+$ calcd for $C_{41}H_{34}N_2O_2S_2$, z = 1 : 650.206 ; found 650.458.

2,7-bis(5-diethylamide-thiophen-2-yl)spiro[cyclopentane-9,9-fluorene]: *dye.spi*C_4**NEt$_2$ (6)**

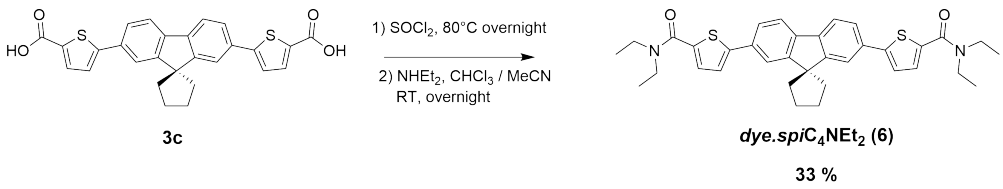

3c

Scheme S6: Synthesis of 2,7-bis(5-diethylamide-thiophen-2-yl)spiro[cyclopentane-9,9-fluorene] : *dye.spi*C_4NEt$_2$ (6)

Diacid **3c** (30 mg, 0.063 mmol, 1 eq.) was dissolved into dry $SOCl_2$(1,5 mL) and heated to reflux overnight. The next day, $SOCl_2$ was evaporated under vacuum with two liquid nitrogen traps. To this yellow product, a mixture of diethylamine (0.020 mL, 0.190 mmol, 3 eq.) and anhydrous DMF (3 mL) were added and stirred for 1 h at RT. The solution was evaporated under reduced pressure at 60°C to remove the DMF. The product was diluted in DCM and then washed with water, a saturated citric acid solution and water again until neutral pH. Then, the organic phases were collected and dried with $MgSO_4$, filtered and evaporated. Finally, the crude was purified on a silica-gel column chromatography using a 80/20 to 70/30 DCM/ACN mixture to yield ***dye.spi*$\mathbf{C_4NEt_2}$ (6)** as a pure yellow solid (20 mg, 33%).

2.2 *d*FONs preparation

5mM solutions of dyes were prepared in DMSO (a good solvent for all dyes) and subsequently diluted in THF, resulting in final stock solutions at 0.5mM (THF/DMSO, 9:1 v/v). 5 mL of distilled water was stirred with a magnetic stir bar at 900 rpm. Subsequently, 50 µL of 0.5mM stock solution of dyes were loaded into a 50 µL Hamilton syringe and added dropwise to the water at a rate of one drop every 10 seconds. The resulting dispersion was stirred for an additional 30 minutes. Finally, the solution was centrifuged at 3000 rpm for 5 minutes at 20 °C and the supernatant was collected.

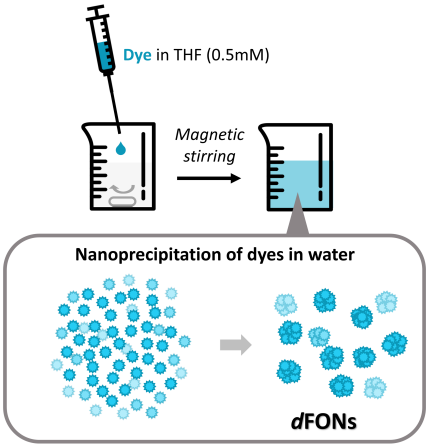

Figure S1: Preparation of *d*FONs by the nanoprecipitation technique

3 Complementary data

3.1 Dyes NMR spectra

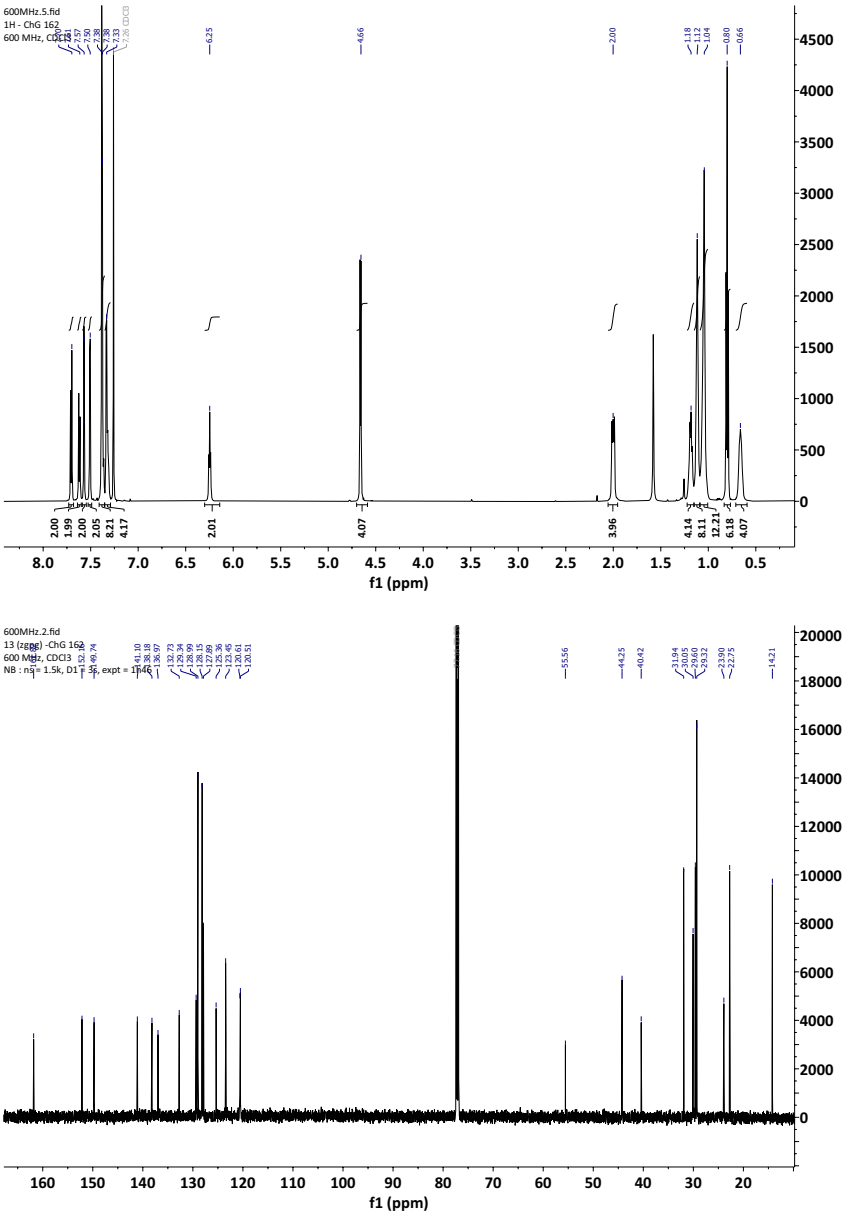

Figure S2: ^{1}H and ^{13}C NMR spectrum of ***dye.n*C$_9$ (5a) in CDCl$_3$**

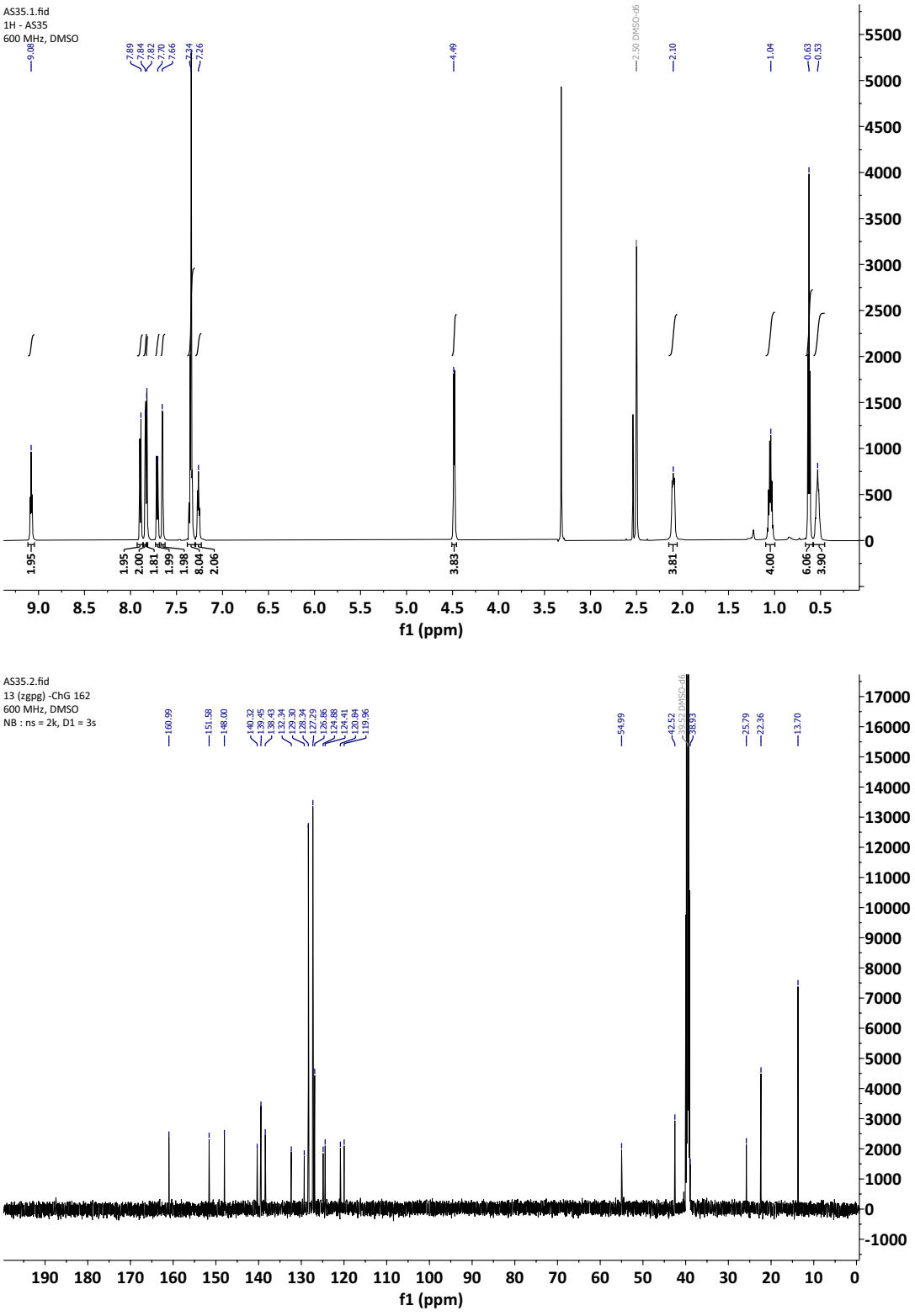

Figure S3: ^{1}H and ^{13}C NMR spectrum of ***dye.n*C$_4$ (5b)** in DMSO-*d6*.

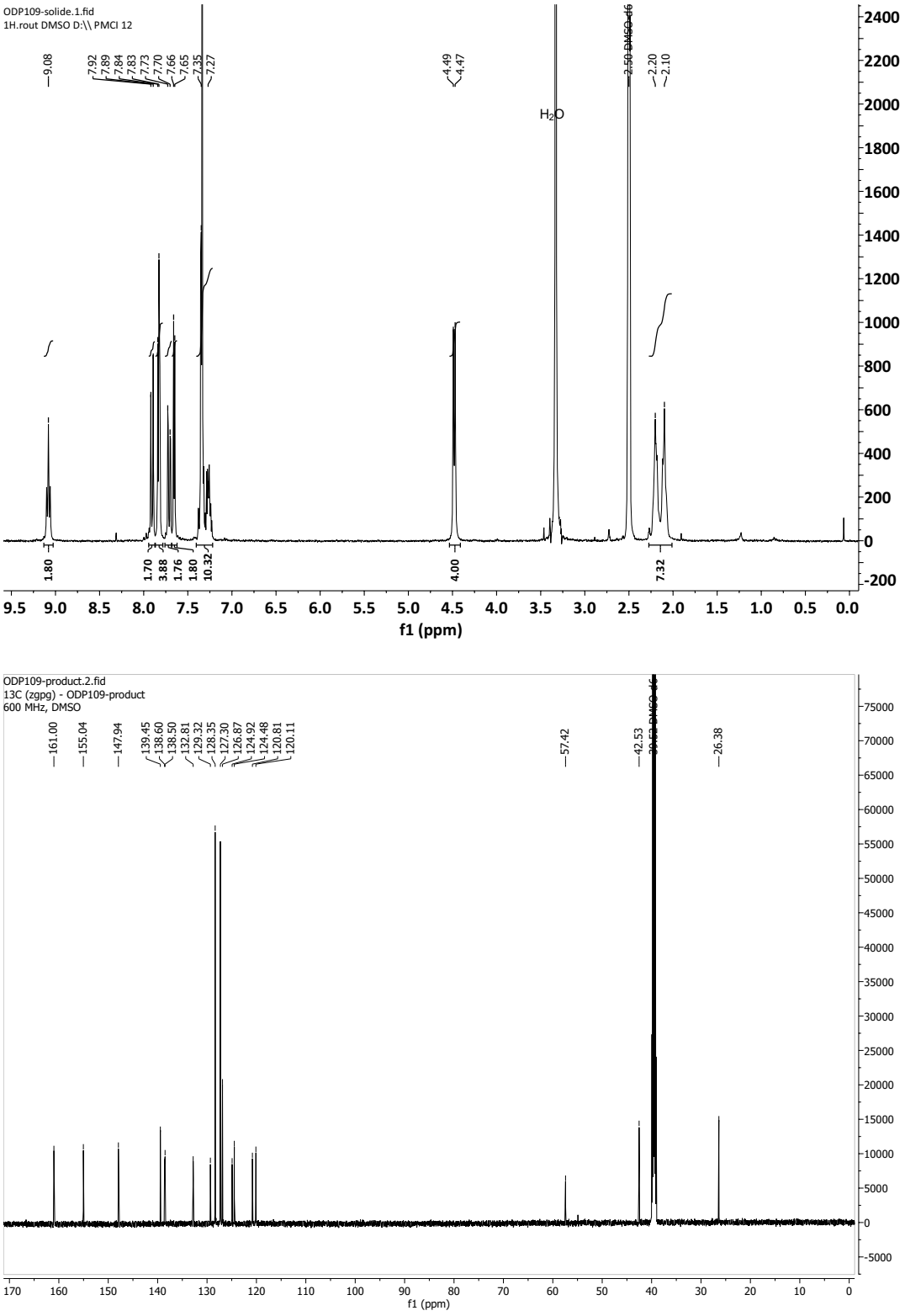

Figure S4: ^{1}H and ^{13}C NMR spectrum of ***dye.spi*C$_4$ (5c)** in DMSO-*d6*

3.2 Complementary photophysics data

3.3 Solvatochromism

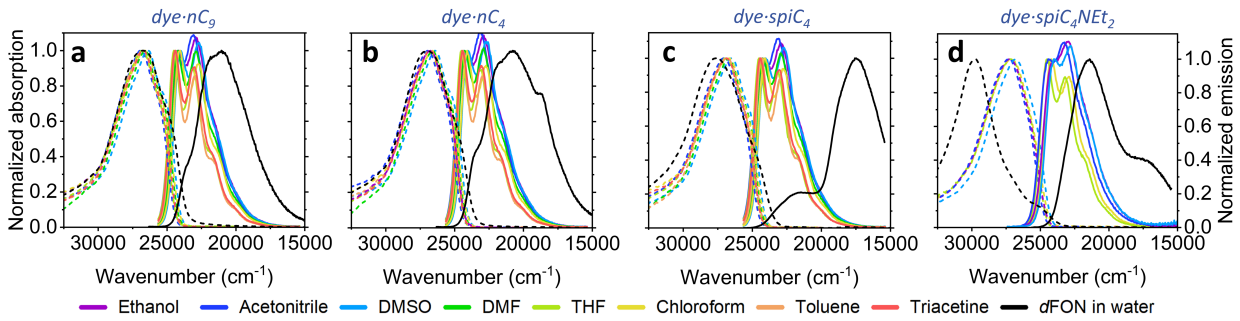

Figure S5: Normalized absorption (dashed line) and emission spectra (solid line) of dyes in various organic solvents, with the corresponding nanoparticles in water for comparison (black): a) *dye*·nC_9, b) *dye*·nC_4, c) *dye*·$spiC_4$, d) *dye*·$spiC_4NEt_2$.

Table S1: Photophysical and structural properties of the three dyes in THF and of the associated *d*FONs in water, at 20°C.

Sample	Solvent	$\lambda_{abs}^{max,\ a)}$	$\varepsilon^{max,\ b)}$	$\Delta_{\nu}^{c)}$	$\lambda_{em}^{max,\ d)}$	$\Phi_F^{e)}$	$\tau_{amp}^{f)}$	$k_r^{g)}$	$k_{nr}^{h)}$	$D_{TEM}^{i)}$	$B^{j)}$	$B_V^{k)}$
		nm	$\times 10^3 M^{-1} cm^{-1}$	cm^{-1}	nm		ns	ns^{-1}	ns^{-1}	nm	$M^{-1} cm^{-1}$	$\times 10^3 M^{-1} cm^{-1} nm^{-3}$
$dye{\cdot}nC_9$	THF	373	69 ± 8	2300	408	0.72 ± 0.02	0.9	0.8	0.3	na	$50 \cdot 10^3$	35
*d*FON($dye{\cdot}nC_9$)	H_2O	374	48 ± 8	5685	475	0.23 ± 0.01	0.5	0.5	1.5	36 ± 16	$19 \cdot 10^7$	8
$dye{\cdot}nC_4$	THF	373	66 ± 2	2360	409	0.65 ± 0.03	0.9	0.7	0.4	na	$43 \cdot 10^3$	36
*d*FON($dye{\cdot}nC_4$)	H_2O	370	44 ± 2	6237	481	0.15 ± 0.01	0.4	0.4	2.1	39 ± 12	$17 \cdot 10^7$	6
$dye{\cdot}spiC_4$	THF	372	68 ± 2	2372	408	0.70 ± 0.03	0.9	0.8	0.3	na	$48 \cdot 10^3$	44
*d*FON($dye{\cdot}spiC_4$)	H_2O	362	34 ± 2	10050	569 (466)	0.03 ± 0.01	0.1/4.8*	0.1/0.01*	10/0.2*	34 ± 6	$1.9 \cdot 10^7$	0.9
$dye{\cdot}spiC_4NEt_2$	THF	368	60 ± 5	2660	408	0.62 ± 0.05	0.8	0.8	0.5	na	na	38
*d*FON($dye{\cdot}spiC_4NEt_2$)	H_2O	336	33 ± 5	8120	462	0.03 ± 0.01	0.6	0.05	1.6	nd	nd	1

(a) Absorbance maximum wavelength ; (b) Molar extinction coefficient of the dyes at λ_{abs}^{max} (in solution in THF or as *d*FONs subunits), measured from three differently prepared solutions and subsequent dilutions (error bars correspond to the standard deviation on all points) ; (c) Stokes shift ; (d) Emission maximum wavelength ; (e) Fluorescence quantum yield, determined by the relative multi-point method, from the slope of integrated emission versus absorbance for a series of dilutions, using references: Quinine bisulfate in H_2SO_4 0.5 M ($\Phi_F = 0.546$)[1] and 4-(dicyanomethylene)-2-methyl-6-[p-(dimethyl-amino) styryl]-4H-pyran in EtOH ($\Phi_F = 0.437$).[2] Error bars correspond to the standard error on the linear regression ; (f) Amplitude-averaged fluorescence lifetime, using $\lambda_{exc} = 370$ nm and $\lambda_{em} = 450$ nm, except for (*): $\lambda_{em} = 590$ nm, ; (g) Radiative rate constant ; (h) Non-radiative rate constant ; (i) Mean dry diameter measured by transmission electron microscopy (error: standard deviation) ; (j) Brightness of the object ; (k) Brightness per volume. ‡Assumed volume for a single dye molecule: 1 nm^3. All steady-state fluorescence emission spectrum were recorded using λ_{exc}=370 nm. na = not appropriated. $dye{\cdot}spiC_4NEt_2$ data were already published in *Dal Pra et al.* Small Methods **2024**.[7]

3.4 Time resolved fluorescence spectroscopy

Table S2: Fluorescence lifetimes of the dyes in THF and as *d*FONs subunits in water at λ_{exc}=370 nm.

dye	solvent	λ_{em} [a]	τ_1 [b]	a_1 [c]	τ_2 [b]	a_2 [c]	τ_3 [b]	a_3 [c]	χ^2 [d]	τ_{int} [e]	τ_{amp} [f]
		nm	ns		ns		ns			ns	ns
$dye{\cdot}nC_9$	THF	408	0.9	1	-	-	-	-	1.10	0.9	0.9
$dye{\cdot}nC_4$	THF	409	0.9	1	-	-	-	-	1.28	0.9	0.9
$dye{\cdot}spiC_4$	THF	408	0.9	1	-	-	-	-	0.89	0.9	0.9
$dye{\cdot}spiC_4NEt_2$	THF	408	0.8	1	-	-	-	-	1.16	0.8	0.8
*d*FON($dye{\cdot}nC_9$)	H_2O	450	0.4	0.060	1.2	0.004	-	-	1.22	0.6	0.5
*d*FON($dye{\cdot}nC_4$)	H_2O	450	0.3	0.059	0.8	0.014	2.4	0.001	0.99	0.6	0.4
*d*FON($dye{\cdot}spiC_4$)	H_2O	450	0.1	0.338	1.1	0.003	-	-	1.33	0.2	0.1
*d*FON($dye{\cdot}spiC_4$)	H_2O	590	2.6	0.013	7.0	0.013	-	-	1.03	5.8	4.8
*d*FON($dye{\cdot}spiC_4NEt_2$)	H_2O	450	0.4	0.043	1.0	0.019	-	-	1.21	0.7	0.6

a) Detection wavelength ; b) τ_i: individual fitted fluorescence lifetimes ; c) a_i: normalized fitted pre-exponential coefficients ; d) Goodness of fit (ideal value: $\chi^2 = 1$) ; e) Intensity-averaged fluorescence lifetime ; f) Amplitude-averaged fluorescence lifetime.

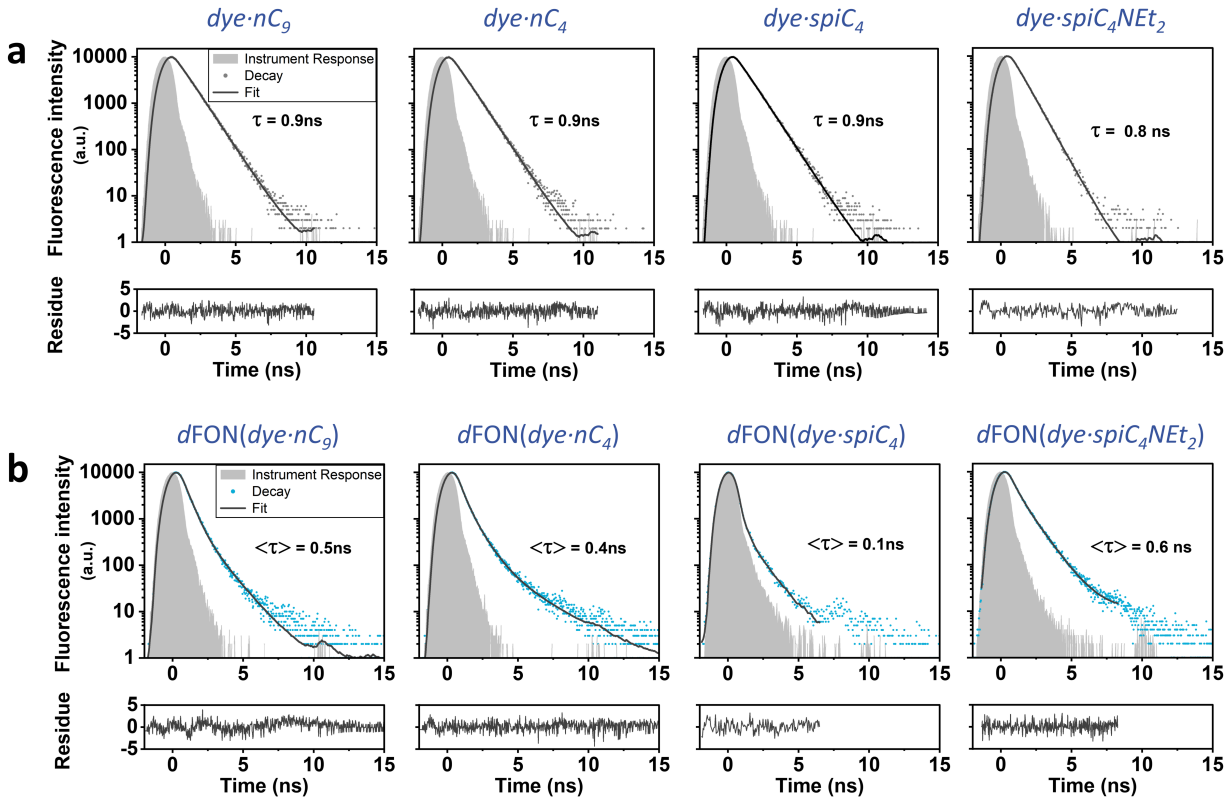

Figure S6: a) Time-resolved fluorescence spectroscopy of $dye{\cdot}nC_9$, $dye{\cdot}nC_4$, $dye{\cdot}spiC_4$ and $dye{\cdot}spiC_4NEt_2$ in THF, using $\lambda_{exc} = 370$ nm and $\lambda_{em} = 408$ nm. The instrument response is shown in light gray, the decay in dark grey and fit with a single exponential function in black. Fit residuals are shown below. Resulting fluorescence lifetime as caption. b) Time-resolved fluorescence spectroscopy of dFON($dye{\cdot}nC_9$), dFON($dye{\cdot}nC_4$), dFON($dye{\cdot}spiC_4NEt_2$) and dFON($dye{\cdot}spiC_4$) in water, using $\lambda_{exc} = 370$ nm and $\lambda_{em} = 450$ nm. The instrument response is shown in light gray, the decay in light blue and fit with a multiexponential function in black. Fit residuals are shown below. Resulting amplitude-averaged fluorescence lifetime as caption.

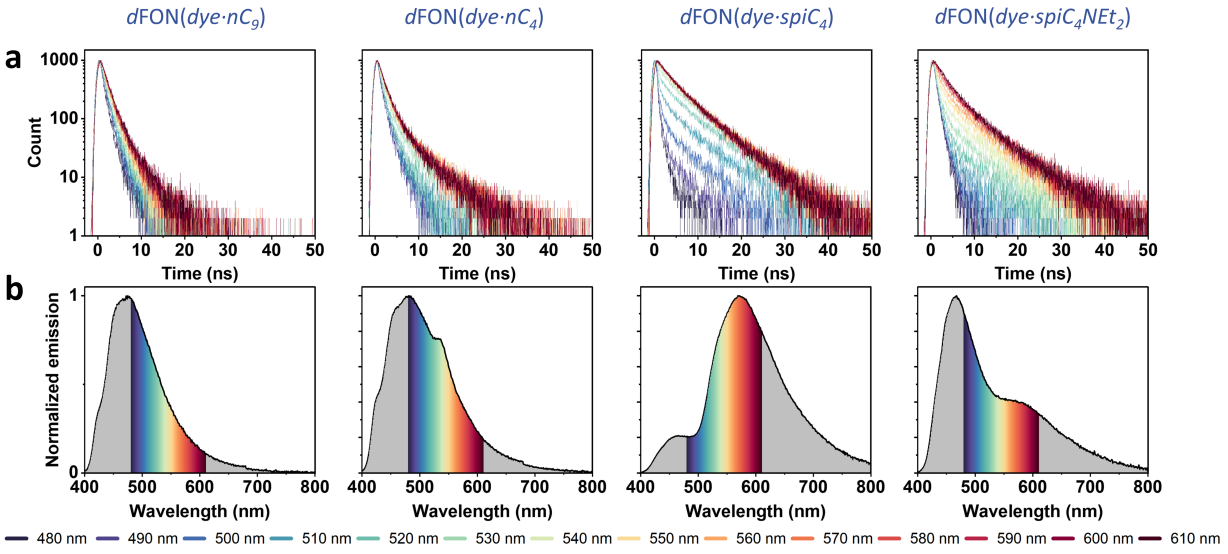

Figure S7: a) Time resolved emission spectra of dFON($dye{\cdot}nC_9$), dFON($dye{\cdot}nC_4$), dFON($dye{\cdot}spiC_4$) and dFON($dye{\cdot}spiC_4NEt_2$) in water, using $\lambda_{exc} = 370$ nm. λ_{em} varies from 480 nm (dark blue) to 610 nm (dark red). b) Steady-state emission spectra of dFONs in water, as a visual guide.

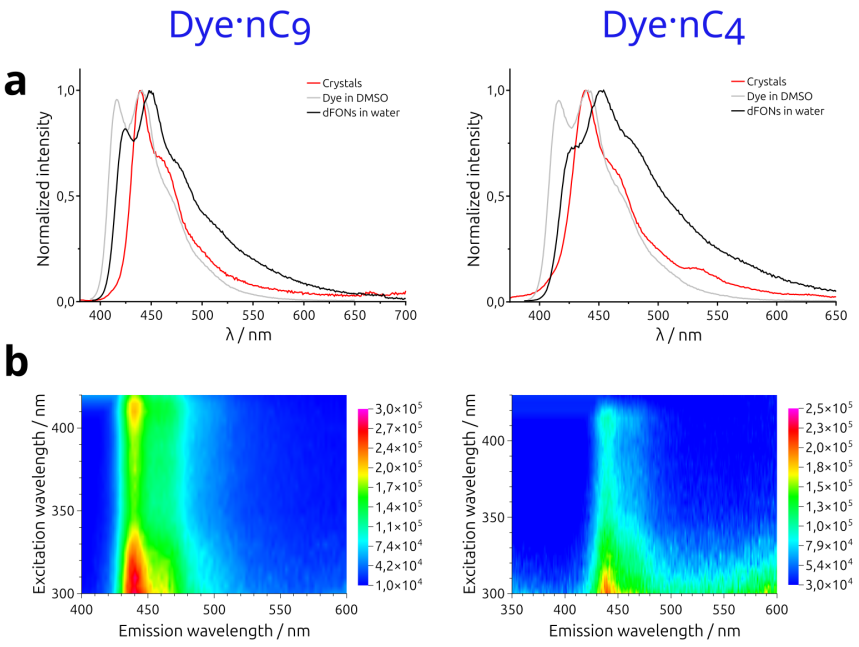

Figure S8: a) Overlay of the fluorescence spectroscopy of dyes $dye{\cdot}nC_9$ and $dye{\cdot}nC_4$ in cristalline form (red), in solution in DMSO (grey) and in water as dFONs (dark). b) 2D excitation and emission map of crystals made of dyes $dye{\cdot}nC_9$ and $dye{\cdot}nC_4$.

3.5 Additional TEM images

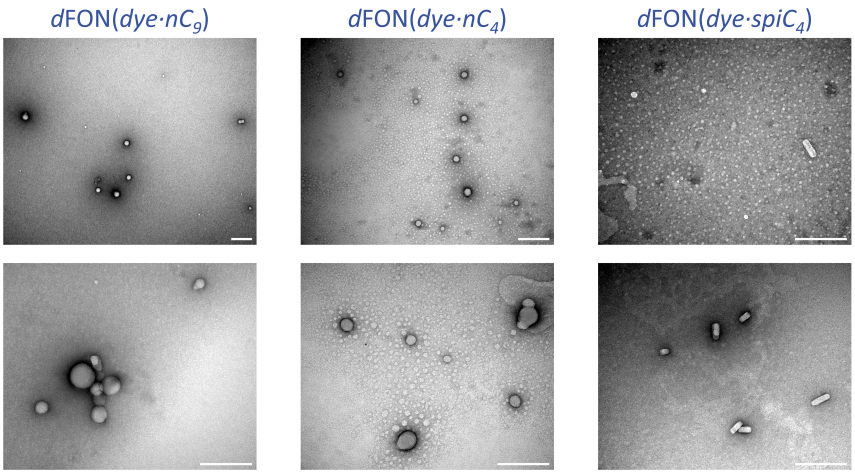

Figure S9: Additional TEM images of dFON($dye{\cdot}nC_9$), dFON($dye{\cdot}nC_4$) and dFON($dye{\cdot}spiC_4$), negatively stained using uranyl acetate.

3.6 Brightness distributions

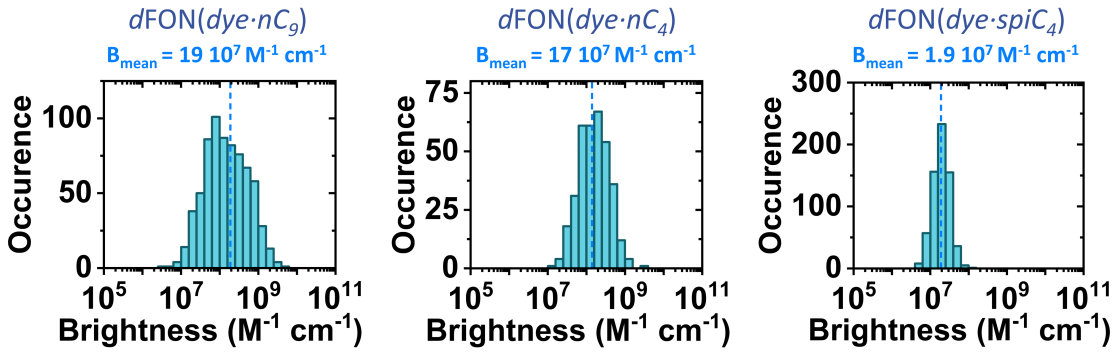

Figure S10: Theoretical brightness distributions of dFON($dye{\cdot}nC_9$), dFON($dye{\cdot}nC_4$) and dFON($dye{\cdot}spiC_4$).

3.7 X-ray analysis

Crystals of $dye{\cdot}nC_4$ and $dye{\cdot}nC_9$ reveal that the benzyl-amide groups adopt a constrained orientation within the crystal lattice, likely due to its interactions with both the thiophene and fluorene units, while the amide groups form hydrogen bonds with the oxygen atoms of the thiophene rings, collectively shaping the molecular arrangement of the dyes.

Table S3: Crystal data and structure refinement for $dye{\cdot}nC_9$

Identification code	$dye{\cdot}nC_9$
Empirical formula	$C_{55}H_{64}N_2O_2S_2$
Formula weight	849.2
Temperature	150(2) K
Wavelength	1.54184 Å
Crystal system	Orthorhombic
Space group	Pbca
Unit cell dimensions	a = 30.466(4) Å, α= 90°. b = 9.8067(14) Å, β= 90°. c = 31.955(8) Å, γ = 90°.
Volume	9547(3) Å3
Z	8
Density (calculated)	1.182 Mg/m^3
Absorption coefficient	1.331 mm^{-1}
F(000)	3648
Crystal size	0.015 x 0.015 x 0.010 mm^3
Theta range for data collection	4.936 to 68.250°.
Index ranges	$-36 \leq h \leq 34$, $-11 \leq k \leq 10$, $-38 \leq l \leq 18$
Reflections collected	21284
Independent reflections	8183 [R(int) = 0.1622]
Completeness to θ = 67.684°	93.70%
Absorption correction	Semi-empirical from equivalents
Max. and min. transmission	1.00000 and 0.90740
Refinement method	Full-matrix least-squares on F^2
Data / restraints / parameters	8183 / 0 / 553
Goodness-of-fit on F^2	0.983
Final R indices [I > 2σ(I)]	R1 = 0.0849, wR2 = 0.1570
R indices (all data)	R1 = 0.2472, wR2 = 0.2163
Extinction coefficient	0.00008(3)
Largest diff. peak and hole	0.317 and -0.390 e.$Å^{-3}$
CCDC number	2524471

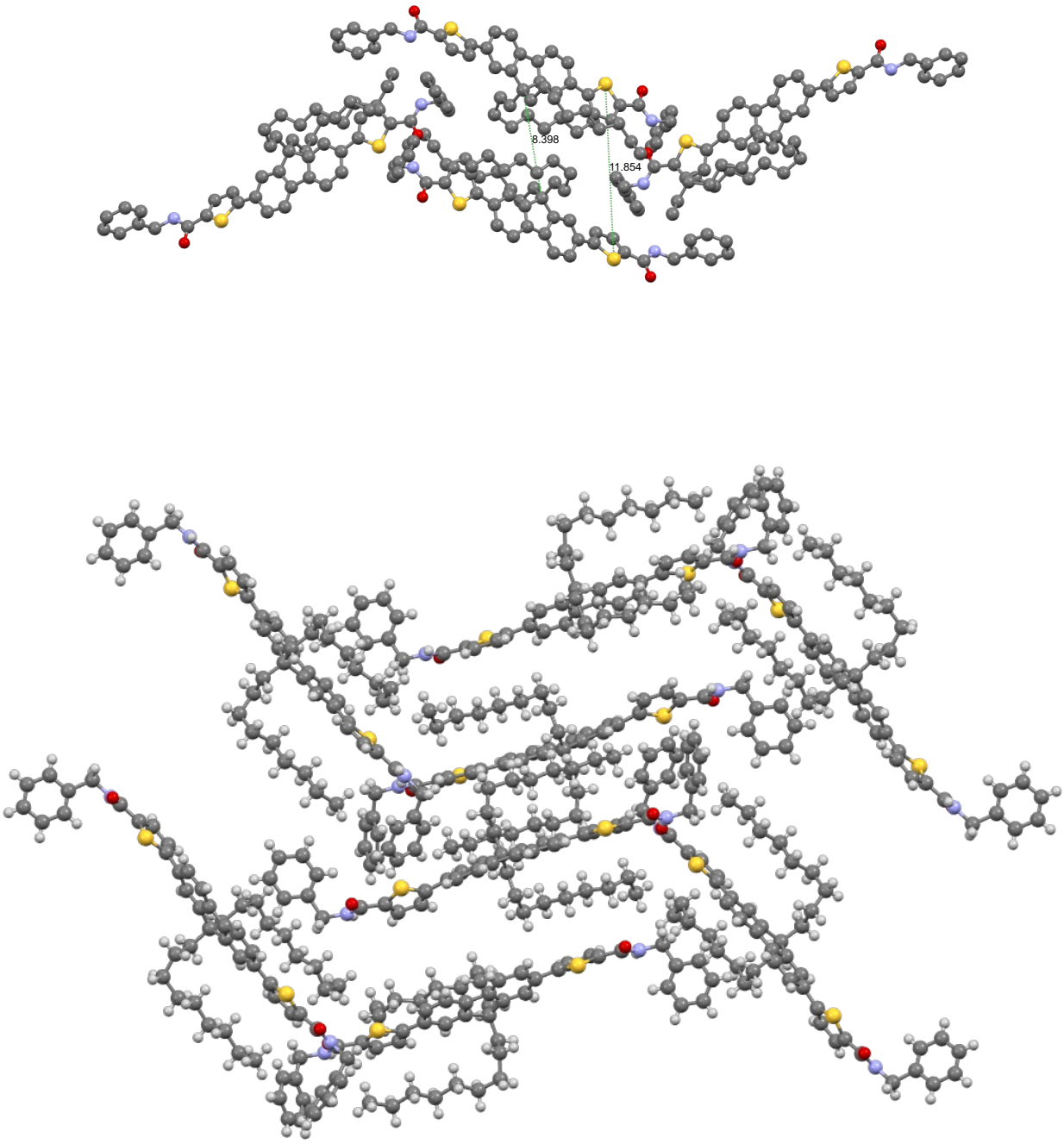

Figure S11: Crystal structure of *dye*·*spi*C_9. Top: only 3 molecules without Hydrogens are represented for clarity. Inter-atomic distances between C1 of two adjacent fluorenes and Sulfur of two thiophenes are indicated in Angstroms. Bottom: full packing.

Table S4: Crystal data and structure refinement for $dye{\cdot}nC_4$

Identification code	$dye{\cdot}nC_4$
Empirical formula	$C_{45}H_{44}N_2O_2S_2$
Formula weight	708.94
Temperature	150(2) K
Wavelength	1.54184 Å
Crystal system	Monoclinic
Space group	$P2_1/c$
Unit cell dimensions	a = 20.2872(9) Å, α= 90°.
	b = 20.8753(10) Å, β= 102.409(4)°.
	c = 9.1499(4) Å, γ = 90°.
Volume	3784.5(3) $Å^3$
Z	4
Density (calculated)	1.244 Mg/m^3
Absorption coefficient	1.582 mm^{-1}
F(000)	1504
Crystal size	0.035 x 0.010 x 0.010 mm^3
Theta range for data collection	3.075 to 68.250°.
Index ranges	$-24 \leq h \leq 18, -25 \leq k \leq 21, -9 \leq l \leq 10$
Reflections collected	17847
Independent reflections	6874 [R(int) = 0.0557]
Completeness to θ = 67.684°	99.30%
Absorption correction	Semi-empirical from equivalents
Max. and min. transmission	1.00000 and 0.93950
Refinement method	Full-matrix least-squares on F2
Data / restraints / parameters	6874 / 0 / 463
Goodness-of-fit on F2	1.007
Final R indices [I > 2σ(I)]	R1 = 0.0490, wR2 = 0.1065
R indices (all data)	R1 = 0.0830, wR2 = 0.1179
Extinction coefficient	0.00044(9)
Largest diff. peak and hole	0.441 and -0.313 e.$Å^{-3}$
CCDC number	2524470

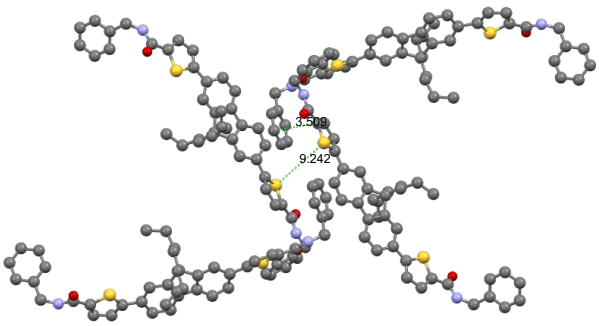

Figure S12: Crystal structure of $dye{\cdot}spiC_4$, not showing Hydrogens. Inter-atomic distances between benzyl and thiophenes and between of Sulfurs of thiophenes are indicated in Angstroms.

3.8 Stability

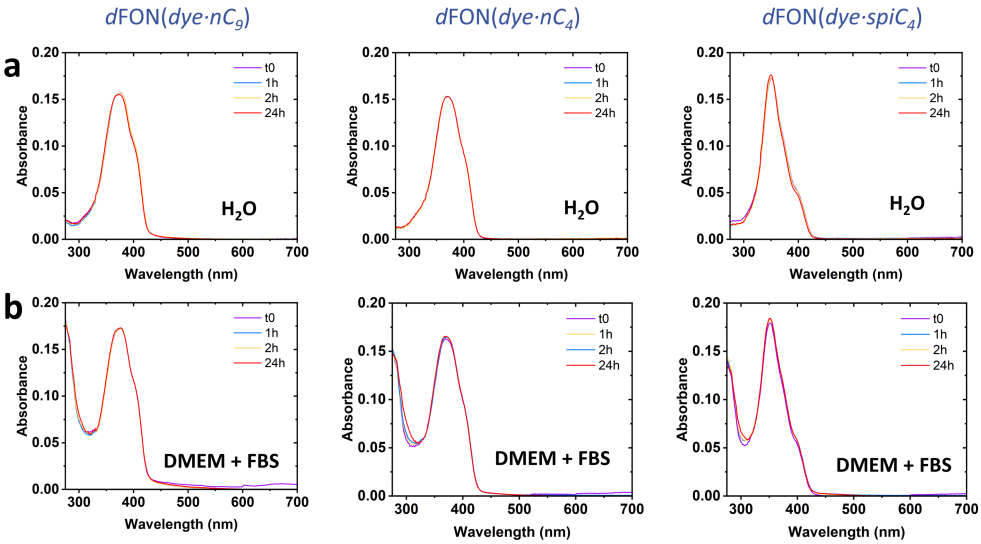

Figure S13: Colloidal stability of *d*FONs. Raw absorbance of *d*FON($dye{\cdot}nC_9$), *d*FON($dye{\cdot}nC_4$) and *d*FON($dye{\cdot}spiC_4$) after 0, 1, 2 and 24h respectively in a) water and b) DMEM with 10% FBS.

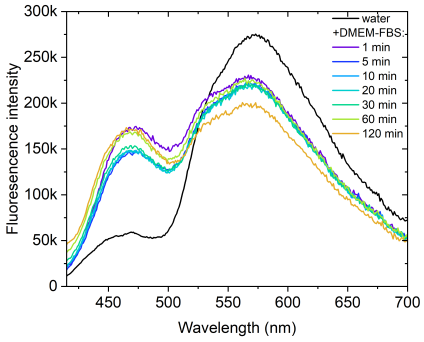

Figure S14: Photophysical stability of *d*FON($dye{\cdot}spiC_4$) in DMEM with 10% FBS over two hours, compared with water. $\lambda_{exc} = 405$ nm.

3.9 Bioimaging

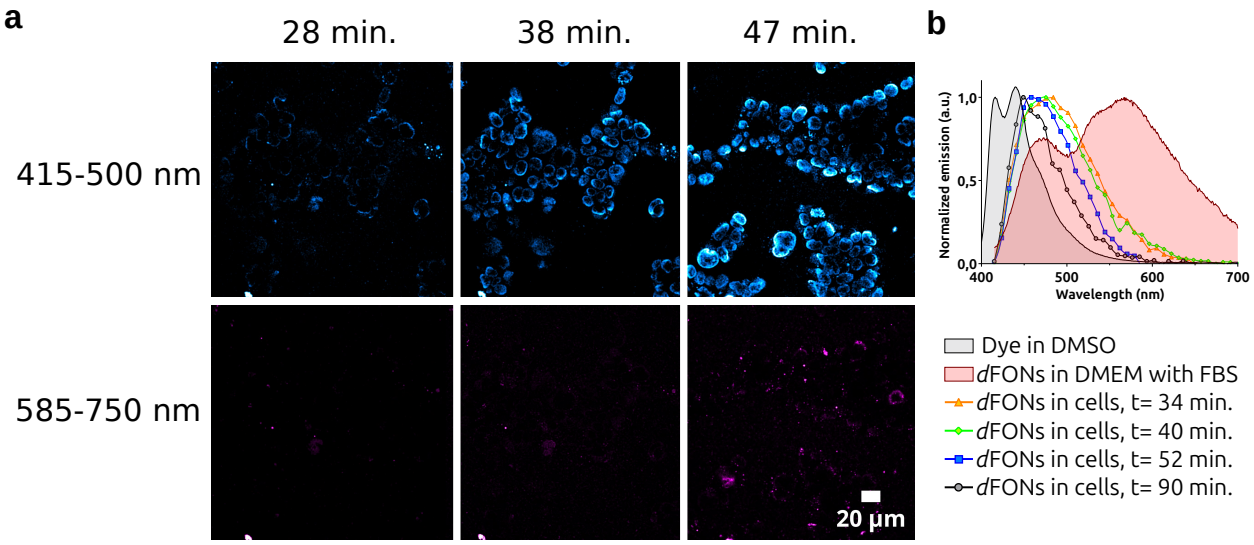

Figure S15: Accumulation of dFON($dye{\cdot}spiC_4$) at 5 nM in live HEK cells in DMEM cell medium monitored by fluorescence imaging. a) The blue channel (top) was acquired with λ_{exc}= 405 nm and λ_{em}=415 - 500 nm. The red channel (bottom) was acquired with λ_{exc}= 405 nm and λ_{em}= 585 - 750 nm. Emission in live cells was recorded at different time after the addition of the dFON($dye{\cdot}spiC_4$) (t= 0 min). For fair comparison, all imaging parameters were the same for all images. b) Normalized emission spectra of dFON($dye{\cdot}spiC_4$) within live cells at different incubation time overlayed with normalized emission of the dFON($dye{\cdot}spiC_4$) in solution in DMEM supplemented with FBS (10%) and of the dye in solution in dimethylsulfoxide (DMSO). Note that datas with incubation time at 90 min weren't acquired on the same petri diches and for this reason the fluorescence imaging is not shown.

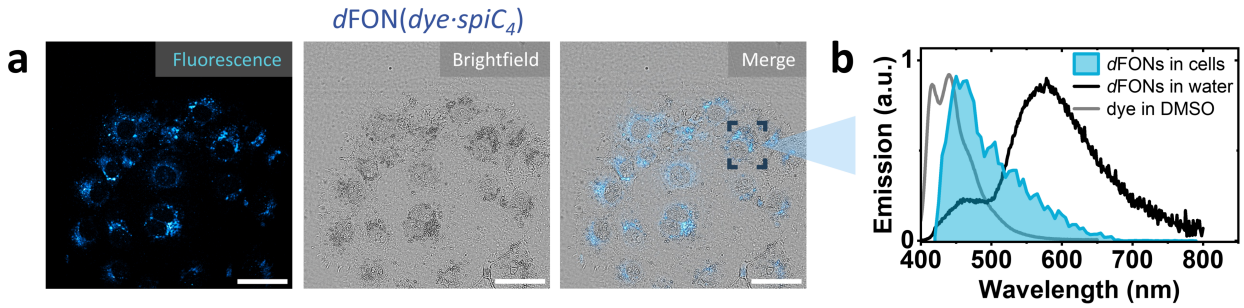

Figure S16: a) Fluorescence microscopy images of COS-7 cells incubated for 2h at 37°C with *d*FON(*dye*·*spiC*$_4$) at 5nM in DMEM cell medium with 10% FBS. Scale bar: 50µm. λ_{exc}= 405 nm, λ_{em}= 420 nm to 795 nm. b) Raw *in cellulo* emission spectrum (lambda scan, λ_{exc}= 405 nm, emission collected from 420 nm to 790 nm in 5 nm steps) of *d*FON(*dye*·*spiC*$_4$) within the cells (blue), overlayed on the normalized emission spectra of *d*FON(*dye*·*spiC*$_4$) in water (black) and of *dye*·*spiC*$_4$ in DMSO (grey).

References

(1) Eaton, D. F. Reference materials for fluorescence measurement. *Pure and Applied Chemistry* **1988**, *60*, 1107–1114.

(2) Rurack, K.; Spieles, M. Fluorescence Quantum Yields of a Series of Red and Near-Infrared Dyes Emitting at 600-1000 nm. *Analytical Chemistry* **2011**, *83*, 1232–1242.

(3) CrysAlis PRO Software, version 1.171.44.122a.

(4) Sheldrick, G. M. A short history of SHELX. *Acta Crystallographica Section A* **2008**, *64*, 112–122.

(5) Farrugia, L. J. WinGX and ORTEP for Windows: an update. *Journal of Applied Crystallography* **2012**, *45*, 849–854.

(6) Macrae, C. F.; Bruno, I. J.; Chisholm, J. A.; Edgington, P. R.; McCabe, P.; Pidcock, E.; Rodriguez-Monge, L.; Taylor, R.; van de Streek, J.; Wood, P. A. Mercury CSD 2.0 – new features for the visualization and investigation of crystal structures. *Journal of Applied Crystallography* **2008**, *41*, 466–470.

(7) Dal Pra, O.; Daniel, J.; Recher, G.; Blanchard-Desce, M.; Grazon, C. Two-photon Dye-Based Fluorogenic Organic Nanoparticles as Intracellular Thiols Sensors. *Small Methods* **2024**, *8*, 2400716.